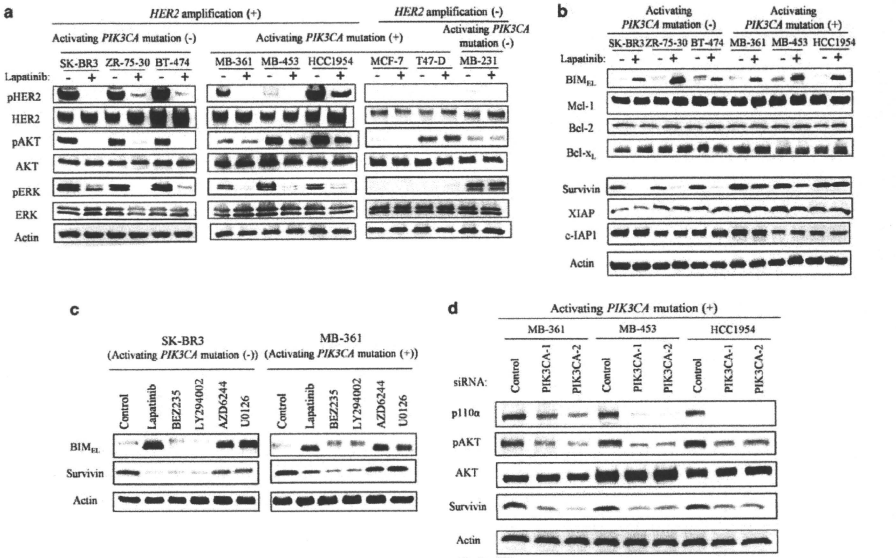

Figure 2 Effects of lapatinib on HER2, AKT and ERK phosphorylation as well as on apoptosis-related protein expression in breast cancer cell lines. (**a**, **b**) The indicated cell lines were incubated with or without lapatinib (1 μM) for 24 h (**a**) or 48 h (**b**), after which cell lysates were prepared and subjected to immunoblot analysis with antibodies to phosphorylated (p) or total forms of HER2, AKT or ERK as well as with those to the indicated apoptosis-related proteins or to β-actin (loading control). The position of the band corresponding to BIM$_{EL}$ is indicated. (**c**) SK-BR3 or MB-361 cells were incubated in the absence (control, 0.1% dimethyl sulfoxide) or presence of lapatinib (1 μM), BEZ235 (0.3 μM), LY294002 (20 μM), AZD6244 (0.3 μM) or U0126 (20 μM) for 48 h, after which cell lysates were prepared and subjected to immunoblot analysis with antibodies to BIM, to survivin or to β-actin. (**d**) The indicated cell lines were transfected with non-specific (control), PIK3CA-1 or PIK3CA-2 siRNAs for 48 h, after which cell lysates were prepared and subjected to immunoblot analysis with antibodies to the indicated proteins.

family of proteins, in *HER2* amplification-positive cells regardless of the *PIK3CA* mutational status, whereas it had little effect on the expression of other Bcl-2 family members, including Mcl-1, Bcl-2 and Bcl-x$_L$. Quantitative reverse transcription and PCR analysis showed that lapatinib increased the amount of BIM mRNA in all *HER2* amplification-positive cells in a manner independent of the *PIK3CA* mutational status (Supplementary Figure 1), suggesting that BIM induction by lapatinib is mediated at the transcriptional level. On the other hand, lapatinib downregulated the expression of survivin, a member of the inhibitor of apoptosis protein (IAP) family, in *HER2* amplification-positive cells without an activating *PIK3CA* mutation but not in those with such a mutation. The expression of other IAP family members, including XIAP and c-IAP1, was not substantially affected by lapatinib in any of the cell lines examined.

To identify the signaling pathways responsible for induction of BIM and downregulation of survivin by lapatinib, we examined the effects of specific inhibitors of PI3K (BEZ235 and LY294002) and of the ERK kinase MEK (AZD6244 and U0126). Each of the MEK inhibitors induced BIM expression without affecting the expression of survivin in *HER2* amplification-positive cells regardless of the *PIK3CA* mutational status (Figure 2c), suggesting that expression of BIM is regulated by the MEK-ERK pathway. Conversely, the PI3K inhibitors reduced the abundance of survivin without affecting that of BIM in all cells with *HER2* amplification (Figure 2c). We further examined the effect of depletion of PIK3CA (p110α) by RNA interference (RNAi) on survivin expression in *PIK3CA* mutant cells. Introduction of two independent small interfering RNAs (siRNAs) specific for PIK3CA mRNA (PIK3CA-1 and PIK3CA-2 siRNAs) into *HER2* amplification-positive cells with an activating *PIK3CA* mutation, resulted in a marked decrease in the expression of p110α and a concomitant decrease in the level of AKT phosphorylation. This depletion of p110α was also associated with downregulation of survivin expression in these cell lines (Figure 2d), suggesting that survivin expression was regulated through the PI3K pathway. Together, these data suggested that lapatinib induced BIM expression through inhibition of the MEK-ERK pathway in *HER2* amplification-positive

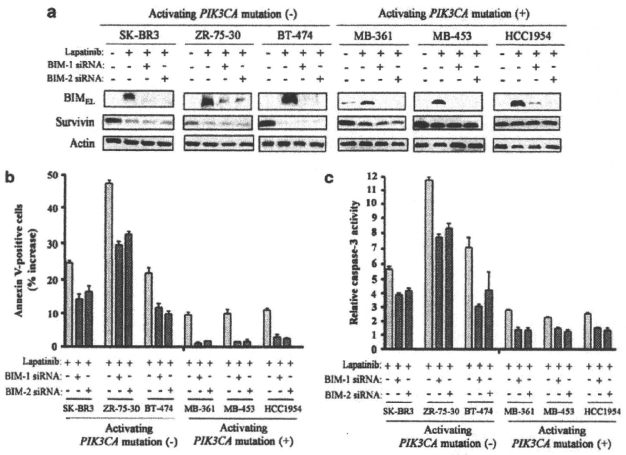

Figure 3 Effect of inhibition of BIM induction on lapatinib-induced apoptosis in *HER2* amplification-positive breast cancer cells with or without an activating *PIK3CA* mutation. (**a**) The indicated cell lines were transfected with BIM-1, BIM-2 or non-specific siRNAs for 24 h and then incubated for 48 h in complete medium with or without lapatinib (1 μM). Cell lysates were then prepared and subjected to immunoblot analysis with antibodies to BIM, to survivin or to β-actin. (**b**) Cells transfected as in a were incubated for 72 h with or without lapatinib (1 μM), and then evaluated for the proportion of apoptotic cells by staining with annexin V and propidium iodide followed by flow cytometry. The percentage increase in the number of apoptotic cells relative to the corresponding value for cells transfected with the control siRNA and incubated without lapatinib is shown. (c) Lysates prepared from cells treated as in (**a**) were assayed for caspase-3 activity, which is expressed relative to the corresponding value for cells transfected with the control siRNA and incubated without lapatinib. Data in b and c are means ± s.e. from three independent experiments.

cells with or without an activating *PIK3CA* mutation. On the other hand, lapatinib downregulated survivin expression through inhibition of the PI3K signaling pathway in *HER2* amplification-positive cells without a *PIK3CA* mutation, but it had little effect on survivin expression in cells with such a mutation, likely as a result of activation of the PI3K pathway by the *PIK3CA* mutation.

Effect of inhibition of BIM induction on lapatinib-induced apoptosis in cells with HER2 *amplification*

To investigate the role of BIM induction in lapatinib-induced apoptosis, we transfected *HER2* amplification-positive cells with two independent siRNAs specific for BIM mRNA (BIM-1 and BIM-2 siRNAs). Each BIM siRNA markedly suppressed the lapatinib-induced upregulation of BIM without affecting lapatinib-induced downregulation of survivin (Figure 3a). The annexin V binding assay showed that such transfection resulted in partial inhibition of lapatinib-induced apoptosis in *HER2* amplification-positive cells without an activating *PIK3CA* mutation, whereas lapatinib-induced apoptosis was almost completely inhibited by BIM siRNA in cells with such a mutation (Figure 3b). Similar to the results of the annexin V binding assay, transfection with BIM siRNA resulted in partial inhibition of the lapatinib-induced activation of caspase-3 in cells without a *PIK3CA* mutation, whereas it resulted in almost complete inhibition of this effect of lapatinib in cells with a *PIK3CA* mutation (Figure 3c). The BH3-mimetic ABT737, which binds to anti-apoptotic Bcl-2 family members, including Bcl-2, Bcl-xl and Bcl-w, was shown to enhance apoptosis under conditions of BIM induction (Cragg *et al*., 2007, 2008; Gong *et al*., 2007). We therefore examined the effect of the combination of lapatinib and ABT737 on induction of apoptosis in *HER2*-amplified breast cancer cells with or without a *PIK3CA* mutation. We found that ABT737 enhanced lapatinib-induced apoptosis both in HER2-positive cells without a *PIK3CA* mutation, and in those with a *PIK3CA* mutation with an average fold increase of 1.20 and 1.48, respectively ($P<0.05$) (Supplementary Figure 2), supporting a role for BIM induction in lapatinib-induced apoptosis. These data thus indicated that BIM induction contributes to lapatinib-induced apoptosis in cells with *HER2* amplification, but that the extent of this contribution differs according to the mutational status of *PIK3CA*.

Combined effect of lapatinib and BEZ235 on apoptosis in HER2 *amplification-positive cells with an activating* PIK3CA *mutation*

Given that lapatinib manifested only a moderate pro-apoptotic effect in cells with an activating *PIK3CA*

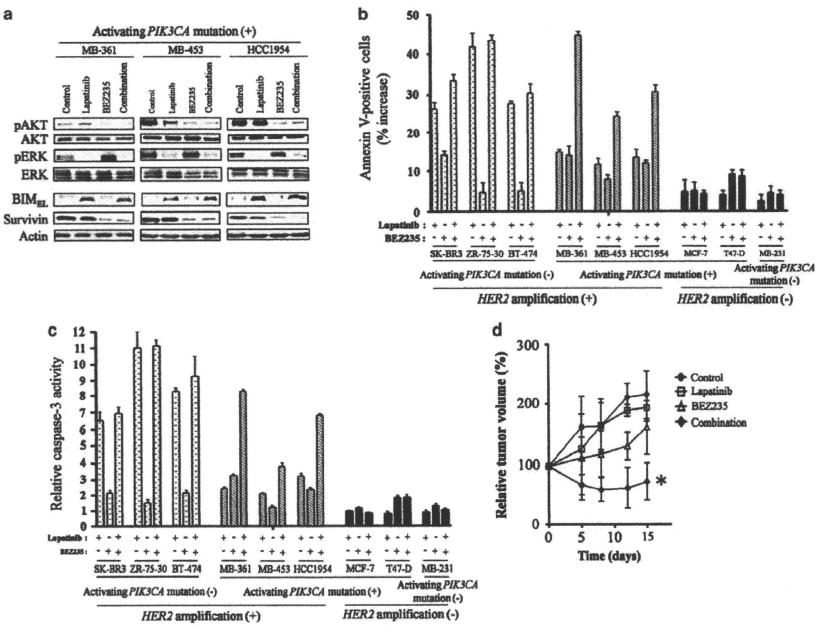

Figure 4 Effects of the combination of BEZ235 and lapatinib in *HER2* amplification-positive cells with an activating *PIK3CA* mutation. (**a**) The indicated cell lines were incubated in the absence (control, 0.1% dimethyl sulfoxide) or presence of lapatinib (1 μM), BEZ235 (0.03 μM) or both agents (combination) for 48 h, after which cell lysates were prepared and subjected to immunoblot analysis with antibodies to the indicated proteins. (**b**) Cells were incubated in the absence or presence of lapatinib (1 μM) or BEZ235 (0.03 μM), as indicated, for 72 h, after which the proportion of apoptotic cells was determined by staining with annexin V and propidium iodide followed by flow cytometry. The percentage increase in the number of apoptotic cells relative to the corresponding value for cells incubated without addition is shown. (**c**) Cells treated as in (**a**) were lysed and assayed for caspase-3 activity, which is expressed relative to the corresponding value for cells incubated without addition. Data in (**b**, **c**) are means ± s.e. from three independent experiments. (**d**) Nude mice with tumor xenografts established by subcutaneous injection of HCC1954 cells were treated daily for 2 weeks with vehicle (control), BEZ235 (15 mg/kg per day), lapatinib (100 mg/kg per day) or the combination of both drugs. Tumor size was determined at the indicated times after treatment onset and is expressed as a percentage of that at time 0. Data are means ± s.e. for six mice per group. *$P < 0.05$ for the combination of BEZ235 and lapatinib versus either BEZ235 or lapatinib alone.

mutation despite the preserved induction of BIM, we hypothesized that insufficient inhibition of the PI3K pathway by lapatinib might be responsible for the limited size of this effect compared with that observed in cells without such a mutation. We therefore examined whether additional inhibition of the PI3K pathway by BEZ235 might enhance the effect of lapatinib on apoptosis in *PIK3CA* mutant cells. Treatment with BEZ235, which was previously shown to inhibit the PI3K pathway in cells expressing activated PIK3CA (Serra *et al*., 2008; Brachmann *et al*., 2009), resulted in marked inhibition of AKT phosphorylation (but not of ERK phosphorylation) in *HER2* amplification-positive cells with an activating *PIK3CA* mutation (Figure 4a). The combination of BEZ235 and lapatinib resulted in inhibition of both AKT and ERK phosphorylation (Figure 4a). Consistent with the notion that regulation of survivin is mediated through the PI3K pathway and that of BIM is mediated through the MEK-ERK pathway, treatment with BEZ235 alone induced down-regulation of survivin expression without affecting BIM expression, whereas the combination of BEZ235 and lapatinib elicited both survivin downregulation and BIM upregulation (Figure 4a). The combination of BEZ235 and lapatinib increased the number of apoptotic cells to an extent markedly greater than that apparent with either agent alone in *HER2* amplification-positive cells with a *PIK3CA* mutation, whereas the effect of lapatinib was similar in the absence or presence of BEZ235 in those without a *PIK3CA* mutation or in cells negative for *HER2* amplification (Figure 4b). A similar pattern was observed for the effects of lapatinib and

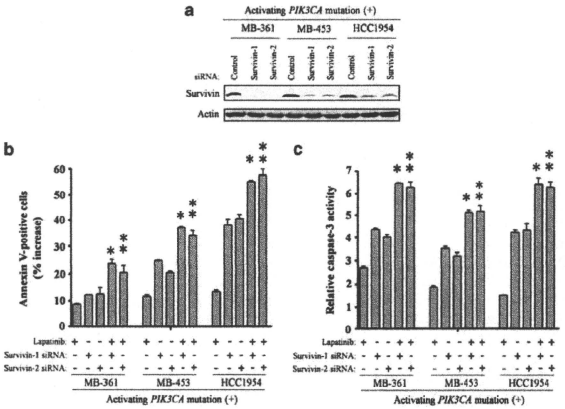

Figure 5 Effect of survivin depletion on apoptosis in *HER2* amplification-positive cells with an activating *PIK3CA* mutation. (**a**) The indicated cell lines were transfected with non-specific (control), survivin-1 or survivin-2 siRNAs for 48 h, after which cell lysates were prepared and subjected to immunoblot analysis with antibodies to survivin or to β-actin. (**b**) Cells transfected as in (**a**) were incubated in complete medium with or without lapatinib (1 μM) for 72 h, after which the proportion of apoptotic cells was determined by staining with annexin V and propidium iodide followed by flow cytometry. The percentage increase in the number of apoptotic cells relative to the corresponding value for cells transfected with the control siRNA and incubated without lapatinib is shown. (**c**) Cells transfected as in (**a**) were incubated with or without lapatinib (1 μM) for 48 h, lysed and assayed for caspase-3 activity, which is expressed relative to the corresponding value for cells transfected with the control siRNA and incubated without lapatinib. Data in (**b**, **c**) are means ± s.e. from three independent experiments. $*P<0.05$ for the combination of lapatinib plus transfection with survivin-1 siRNA versus either treatment alone. $**P<0.05$ for the combination of lapatinib plus transfection with survivin-2 siRNA versus either treatment alone.

BEZ235 on caspase-3 activity (Figure 4c). We further examined the effect of combined treatment with BEZ235 and lapatinib on the growth *in vivo* of *HER2* amplification-positive breast cancer cells with a *PIK3CA* mutation. At the completion of the experiments, tumors treated with either control or lapatinib alone had doubled in size, whereas the combination of lapatinib and BEZ235 maintained tumor regression ($P<0.05$) (Figure 4d), consistent with the combined effect of these agents observed in our *in vitro* experiments. All treatments were well tolerated by the mice, with no signs of toxicity or weight loss during therapy (data not shown). These results thus suggested that effective inhibition of the PI3K pathway and lapatinib treatment cooperate to elicit a substantial level of apoptosis that is accompanied by BIM induction and survivin down-regulation in *HER2* amplification-positive cells with an activating *PIK3CA* mutation.

Combined effect of lapatinib and depletion of survivin on apoptosis in HER2 *amplification-positive cells with an activating* PIK3CA *mutation*

Finally, to investigate the effect of downregulation of survivin expression on apoptosis in *HER2* amplification-positive cells with an activating *PIK3CA* mutation, we depleted such cells of survivin by RNAi (Figure 5a). Each of two independent survivin siRNAs induced apoptosis in these cells, whereas the combination of survivin depletion and lapatinib increased the number of apoptotic cells to an extent significantly greater than that observed with either treatment alone (Figure 5b). These effects on the number of apoptotic cells were confirmed by measurement of caspase-3 activity (Figure 5c). These data thus suggested that down-regulation of survivin itself has a pro-apoptotic effect in cells with a *PIK3CA* mutation, but that survivin depletion and lapatinib cooperate to induce an enhanced level of apoptosis.

Discussion

HER2 amplification is a frequent molecular abnormality in breast cancer, and is associated with a poor outcome and aggressiveness of the disease (Slamon *et al.*, 1987, 1989). Lapatinib, a dual tyrosine kinase inhibitor of EGFR and HER2, shows anti-tumor activity in HER2-overexpressing breast cancer (Geyer *et al.*, 2006; Konecny *et al.*, 2006; Gomez *et al.*, 2008), but the precise mechanism of its anti-tumor effect has remained unclear. We have now investigated the downstream mediators of lapatinib-induced apoptosis in breast cancer cells with *HER2* amplification. BIM is a key pro-apoptotic member of the Bcl-2 family of proteins,

and initiates apoptosis signaling by binding to and antagonizing the function of pro-survival Bcl-2 family members (Chen *et al*., 2005). Our results indicate that lapatinib induces upregulation of BIM expression in *HER2* amplification-positive cells, and that depletion of BIM by RNAi results in marked inhibition of lapatinib-induced apoptosis in these cells. These data suggest that upregulation of BIM expression contributes to the induction of apoptosis by lapatinib in breast cancer cells with *HER2* amplification. We found that BIM induction by lapatinib occurred in *HER2* amplification-positive cells regardless of *PIK3CA* mutational status and was associated with inhibition of ERK phosphorylation. With the use of specific inhibitors of MEK, we also found that regulation of BIM expression is mediated by the MEK-ERK signaling pathway. These findings are consistent with those of previous studies showing that MEK inhibitors induce BIM expression in B-RAF mutant cells (Cragg *et al*., 2008), and that inhibition of the MEK-ERK pathway contributes to BIM induction by EGFR tyrosine kinase inhibitors in non-small cell lung cancer (Costa *et al*., 2007; Cragg *et al*., 2007; Gong *et al*., 2007), and that such upregulation of BIM has an essential role in the induction of apoptosis by these agents. We also found that ABT737 enhanced the induction of apoptosis by lapatinib in cells with *HER2* amplification regardless of *PIK3CA* mutational status, further supporting a role for BIM induction in lapatinib-induced apoptosis. To our knowledge, the present study is the first to show that induction of BIM through inhibition of the MEK-ERK pathway is required for lapatinib-induced apoptosis in breast cancer with *HER2* amplification.

Although lapatinib-induced upregulation of BIM expression occurred in a manner independent of *PIK3CA* mutational status, the pro-apoptotic effect of lapatinib was less pronounced in cells with an activating *PIK3CA* mutation than in those without one. Given that such *PIK3CA* mutations result in hyperactivation of the PI3K signaling pathway (Isakoff *et al*., 2005; Zhao *et al*., 2005; Berns *et al*., 2007), we examined whether activation of this pathway was associated with this difference in the extent of apoptosis. Indeed, we found that lapatinib did not inhibit the phosphorylation of AKT in *HER2* amplification-positive cells with an activating *PIK3CA* mutation. We therefore examined the effect of specific inhibitors of the PI3K pathway on lapatinib-induced apoptosis in cells with a *PIK3CA* mutation. Treatment with BEZ235 effectively inhibited AKT phosphorylation, and the combination of BEZ235 and lapatinib thus inhibited both AKT and ERK phosphorylation and had a pro-apoptotic effect that was markedly greater than that observed with either agent alone. Consistent with these *in vitro* experiments, the combination of lapatinib and BEZ235 exhibits an enhanced anti-tumor effect *in vivo* with HER2-positive xenografts with a *PIK3CA* mutation. These results suggest that additional inhibition of the PI3K pathway is required for effective induction of apoptosis by lapatinib in cells with a *PIK3CA* mutation. Lapatinib shows clinical efficacy both alone and in combination with chemotherapeutic agents, but not all patients with *HER2* amplification-positive tumors respond to such treatment (Slamon *et al*., 1987; Slamon, 1990; Geyer *et al*., 2006; Di Leo *et al*., 2008; Gomez *et al*., 2008). *PIK3CA* mutations have been detected in 20–30% of breast cancer patients with *HER2* amplification (Saal *et al*., 2005; Stemke-Hale *et al*., 2008), and our data now suggest that activation of the PI3K signaling pathway associated with the presence of a *PIK3CA* mutation may be responsible, at least in part, for the limited efficacy of lapatinib in patients with tumors positive for both *HER2* amplification and a *PIK3CA* mutation. Similar to the effects of lapatinib, the MEK inhibitor AZD6244 inhibited ERK phosphorylation and increased BIM expression, without affecting AKT phosphorylation or survivin expression, and it cooperated with BEZ235 to induce apoptosis in *HER2* amplification-positive cells with a *PIK3CA* mutation (Supplementary Figure 3). These data thus indicate the importance of simultaneous interruption of the PI3K-survivin and MEK-ERK-BIM pathways for effective induction of apoptosis in such cells. However, the extent of apoptosis induced by AZD6244 alone or in combination with BEZ235 was less pronounced than that induced by lapatinib, suggesting that the anti-tumor effect of lapatinib in these cells is not mediated exclusively through inhibition of MEK-ERK signaling. Further investigation is thus needed to clarify the relationship of *PIK3CA* mutational status to the efficacy of lapatinib. The development of PI3K inhibitors has advanced substantially in recent years, and clinical trials of these agents alone or in combination with other anti-tumor agents are under way. Our study therefore provides a rationale for clinical evaluation of combination therapy with lapatinib and a PI3K inhibitor in breast cancer patients with *HER2* amplification and a *PIK3CA* mutation.

Survivin is essential for proper completion of various stages of cell division, with this protein having been found to contribute to centrosomal function, spindle formation and kinetochore attachment to spindle microtubules (Speliotes *et al*., 2000; Uren *et al*., 2000). Survivin is preferentially expressed during the mitotic phase of the cell cycle and is physically associated with the mitotic apparatus. It has also been found to be overexpressed in some tumors, with such overexpression having been associated with a poor clinical outcome (Ambrosini *et al*., 1997; Tanaka *et al*., 2000; Altieri, 2003). Like other members of the IAP family such as XIAP and c-IAP1, survivin contains a single BIR (baculoviral IAP repeats) domain. Molecular antagonists of survivin, including anti-sense and siRNA oligonucleotides as well as dominant negative mutants, have been shown to induce apoptosis (Olie *et al*., 2000; Kanwar *et al*., 2001), suggestive of an association between survivin and apoptosis. Consistent with these previous findings, we have now shown that depletion of survivin by two independent siRNAs specific for survivin mRNA increased the number of apoptotic cells and the activity of caspase-3 in *HER2* amplification-positive breast cancer cells with a *PIK3CA* mutation. With the use of siRNAs specific for PIK3CA mRNA,

we further showed that survivin expression is regulated by the PI3K signaling pathway, consistent with previous studies linking survivin expression to this signaling pathway (McKenzie *et al.*, 2010; Peirce *et al.*, 2010). Our finding that survivin downregulation through inhibition of PI3K signaling was associated with the induction of apoptosis, is consistent with the key role of this signaling pathway in cell survival. We found that lapatinib downregulated survivin expression in association with the induction of apoptosis in *HER2* amplification-positive cells without an activating *PIK3CA* mutation. In contrast, expression of survivin was not markedly affected by lapatinib in cells harboring such a *PIK3CA* mutation. We therefore examined the effect of inhibition of survivin expression on lapatinib-induced apoptosis in *PIK3CA* mutant cells. In such cells, the combination of survivin depletion by RNAi and lapatinib treatment exhibited a pro-apoptotic effect markedly greater than that observed with either approach alone, suggesting that downregulation of survivin promotes lapatinib-induced apoptosis. We also found that, unlike lapatinib, the PI3K inhibitor BEZ235 induced downregulation of survivin expression in cells with an activating *PIK3CA* mutation, suggesting that this effect contributes, at least in part, to the enhanced level of apoptosis induced by the combination of lapatinib and BEZ235. Insufficient inhibition of the PI3K-survivin pathway may thus account for the smaller pro-apoptotic effect of lapatinib in *HER2* amplification-positive cells with an activating *PIK3CA* mutation compared with that observed in those without such a mutation.

In conclusion, we have shown that both induction of BIM and inhibition of survivin have a role in lapatinib-induced apoptosis in *HER2* amplification-positive breast cancer cells. Moreover, both the PI3K-survivin pathway and the MEK-ERK-BIM pathway contribute independently to the induction of apoptosis in these cells regardless of *PIK3CA* mutational status. Our data thus show that simultaneous interruption of the PI3K-survivin and MEK-ERK-BIM pathways is required for effective induction of apoptosis in breast cancer cells with *HER2* amplification. They further provide a rationale for the development of new therapeutic strategies for patients with breast tumors positive for *HER2* amplification, including those with an activating *PIK3CA* mutation.

Materials and methods

Cell culture and reagents

The human breast cancer cell lines SK-BR3, ZR-75-30, BT-474, MB-361, MB-453, HCC1954, MCF-7, T47-D and MB-231 were obtained from American Type Culture Collection (Manassas, VA, USA). SK-BR3 cells were cultured in McCoy's medium (Invitrogen, Carlsbad, CA, USA) supplemented with 10% fetal bovine serum; BT-474 cells in Dulbecco's modified Eagle's medium (Invitrogen) supplemented with 10% fetal bovine serum; MB-361, MB-453 and MB-231 cells in L15 medium (Invitrogen) supplemented with 10% fetal bovine serum; and the remaining cells in RPMI 1640 medium (Sigma, St Louis, MO, USA) supplemented with 10% fetal bovine serum. All cells were maintained under a humidified atmosphere of 5% CO_2 at 37 °C. Lapatinib was obtained from Sequoia Research Products (Pangbourne, UK), AZD6244 was from ShangHai Biochempartner (Shanghai, China) and LY294002 and U0126 were from Cell Signaling Technology (Danvers, MA, USA). BEZ235 was kindly provided by Novartis (Basel, Switzerland). MB-453 and HCC1954 cells were found to harbor an H1047 hotspot mutation, and MB-361 cells were found to contain an E545K hotspot mutation by sequencing of exons 9 and 20 of *PIK3CA* (Hoeflich *et al.*, 2009; Kataoka *et al.*, 2010; Saal *et al.*, 2005; Samuels *et al.*, 2004). We categorized BT-474 cells as negative for an activating *PIK3CA* mutation for this study on the basis of the demonstrated lack of transforming activity for the K111N mutation and its minimal effect on downstream signaling (Gymnopoulos *et al.*, 2007; Zhang *et al.*, 2008).

Growth inhibition assay in vitro

Cells were plated in 96-well flat-bottomed plates and cultured for 24 h before exposure to various concentrations of lapatinib for 72 h. TetraColor One (5 mM tetrazolium monosodium salt and 0.2 mM 1-methoxy-5-methyl phenazinium methylsulfate; Seikagaku, Tokyo, Japan) was then added to each well, and the cells were incubated for 3 h at 37 °C before measurement of absorbance at 490 nm with a Multiskan Spectrum instrument (Thermo Labsystems, Boston, MA, USA). Absorbance values were expressed as a percentage of that for untreated cells, and the concentration of lapatinib resulting in 50% growth inhibition (IC_{50}) was calculated.

Annexin V binding assay

Binding of annexin V to cells was measured with the use of an Annexin-V-FLUOS Staining Kit (Roche, Basel, Switzerland). Cells were harvested by exposure to trypsin-EDTA, washed with phosphate-buffered saline and centrifuged at 200 *g* for 5 min. The cell pellets were resuspended in 100 µl of Annexin-V-FLUOS labeling solution, incubated for 10–15 min at 15–25 °C and then analyzed for fluorescence with a flow cytometer (FACSCalibur) and Cell Quest software (Becton Dickinson, Franklin Lakes, NJ, USA).

Clonogenicity assay

Cells were seeded in triplicate in six-well plates and cultured for 48 h in the presence of lapatinib (1 µM) or vehicle. They were then cultured in drug-free medium for 14 days, fixed with methanol:acetic acid (10:1, v/v) and stained with crystal violet. The mean percentage cell survival relative to controls was determined from triplicate wells.

Immunoblot analysis

Cells were washed twice with ice-cold phosphate-buffered saline and then lysed in a solution containing 20 mM Tris-HCl (pH 7.5), 150 mM NaCl, 1 mM EDTA, 1% Triton X-100, 2.5 mM sodium pyrophosphate, 1 mM phenylmethylsulfonyl fluoride and leupeptin (1 µg/ml). The protein concentration of cell lysates was determined with a BCA protein assay kit (Thermo Fischer Scientific, Waltham, MA, USA), and equal amounts of protein were subjected to SDS–polyacrylamide gel electrophoresis on a 7.5 or 12% gel (Bio-Rad, Hercules, CA, USA). The separated proteins were transferred to a nitrocellulose membrane, which was then incubated with Blocking One solution (Nacalai Tesque, Kyoto, Japan) for 20 min at room temperature before incubation overnight at 4 °C with primary antibodies. Rabbit polyclonal antibodies to human phosphorylated HER2 (pY1248), to phosphorylated AKT, to

AKT, to BIM, to Mcl-1, to Bcl-2, to Bcl-x_L, to XIAP and to p110α were obtained from Cell Signaling Technology; those to phosphorylated ERK and to ERK were from Santa Cruz Biotechnology (Santa Cruz, CA, USA); those to c-IAP1 were from R&D Systems (Minneapolis, MN, USA); those to HER2 were from Millipore (Billerica, MA, USA); those to survivin were from Novus (Littleton, CO, USA); and those to β-actin were from Sigma. All antibodies were used at a 1:1000 dilution, with the exception of those to β-actin (1:200). The membrane was then washed with phosphate-buffered saline containing 0.05% Tween 20 before incubation for 1 h at room temperature with horseradish peroxidase-conjugated goat antibodies to rabbit immunoglobulin G (Sigma). Immune complexes were finally detected with chemiluminescence reagents (GE Healthcare, Little Chalfont, UK).

Gene silencing

Cells were plated at 50–60% confluence in six-well plates or 25-cm^2 flasks and then incubated for 24 h before transient transfection for the indicated times with siRNAs mixed with the Lipofectamine reagent (Invitrogen). The siRNAs specific for PIK3CA (PIK3CA-1, 5′-UCAACUUCUUCAAGAUGAA-3′; PIK3CA-2, 5′-GUAGAAUGUUUACUACCAA-3′), BIM (BIM-1, 5′-GGAGGGUAUUUUUGAAUAA-3′; BIM-2, 5′-AGGAGGGUAUUUUUGAAUA-3′), or survivin (survivin-1, 5′-GAAGCAGUUUGAAGAAUUA-3′; survivin-2, 5′-AGAAGCAGUUUGAAGAAUU-3′) mRNAs as well as non-specific (control) siRNAs were obtained from Nippon EGT (Toyama, Japan).

Assay of caspase-3 activity

The activity of caspase-3 in cell lysates was measured with the use of a CCP32/Caspase-3 Fluometric Protease Assay Kit (MBL, Woburn, MA, USA). Fluorescence attributable to cleavage of the Asp–Glu–Val–Asp–7-amino-4-trifluoromethyl coumarin (DEVD-AFC) substrate was measured at excitation and emission wavelengths of 390 and 460 nm, respectively.

Growth inhibition assay in vivo

All animal studies were done with the Recommendations for Handling of Laboratory Animals for biochemical Research compiled by the Committee on Safety and Ethical Handling Regulations for Laboratory Animal Experiments, Kinki University. Cubic fragments of tumor tissue (~2 by 2 by 2 mm) formed by HCC1954 cells were implanted subcutaneously into the axilla of 5–6-week-old male athymic nude mice. When their tumors became palpable, mice were divided in to four groups and treated with vehicle, BEZ235 alone, lapatinib alone and the combination of BEZ235 and lapatinib. Each treatment group contained six mice. BEZ235 and lapatinib were administered by oral gavage daily for 14 days; control animals received a 0.5% (w/v) aqueous solution of hydroxypropylmethylcellulose as vehicle. Tumor volume was determined from caliper measurements of tumor length (L) and width (W) according to the formula $LW^2/2$. Both tumor size and body weight were measured twice per week.

Statistical analysis

Quantitative data from *in vitro* experiments are presented as means ± s.e. from three independent experiments, and were analyzed with the unpaired two-tailed Student's t-test. *In vivo* data are presented as means ± s.e. from six mice and were analyzed by the unpaired two-tailed Student's t-test. A P-value of <0.05 was considered statistically significant.

Conflict of interest

The authors declare no conflict of interest.

Acknowledgements

We thank E Hatashita, K Kuwata, and H Yamaguchi for technical assistance.

References

Altieri DC. (2003). Validating survivin as a cancer therapeutic target. *Nat Rev Cancer* **3**: 46–54.

Ambrosini G, Adida C, Altieri DC. (1997). A novel anti-apoptosis gene, survivin, expressed in cancer and lymphoma. *Nat Med* **3**: 917–921.

Berns K, Horlings HM, Hennessy BT, Madiredjo M, Hijmans EM, Beelen K *et al.* (2007). A functional genetic approach identifies the PI3K pathway as a major determinant of trastuzumab resistance in breast cancer. *Cancer Cell* **12**: 395–402.

Brachmann SM, Hofmann I, Schnell C, Fritsch C, Wee S, Lane H *et al.* (2009). Specific apoptosis induction by the dual PI3K/mTor inhibitor NVP-BEZ235 in HER2 amplified and PIK3CA mutant breast cancer cells. *Proc Natl Acad Sci USA* **106**: 22299–22304.

Burris III HA, Taylor CW, Jones SF, Koch KM, Versola MJ, Arya N *et al.* (2009). A phase I and pharmacokinetic study of oral lapatinib administered once or twice daily in patients with solid malignancies. *Clin Cancer Res* **15**: 6702–6708.

Chen L, Willis SN, Wei A, Smith BJ, Fletcher JI, Hinds MG *et al.* (2005). Differential targeting of prosurvival Bcl-2 proteins by their BH3-only ligands allows complementary apoptotic function. *Mol Cell* **17**: 393–403.

Costa DB, Halmos B, Kumar A, Schumer ST, Huberman MS, Boggon TJ *et al.* (2007). BIM mediates EGFR tyrosine kinase inhibitor-induced apoptosis in lung cancers with oncogenic EGFR mutations. *PLoS Med* **4**: 1669–1679; discussion 1680.

Cragg MS, Jansen ES, Cook M, Harris C, Strasser A, Scott CL. (2008). Treatment of B-RAF mutant human tumor cells with a MEK inhibitor requires Bim and is enhanced by a BH3 mimetic. *J Clin Invest* **118**: 3651–3659.

Cragg MS, Kuroda J, Puthalakath H, Huang DC, Strasser A. (2007). Gefitinib-induced killing of NSCLC cell lines expressing mutant EGFR requires BIM and can be enhanced by BH3 mimetics. *PLoS Med* **4**: 1681–1689; discussion 1690.

Di Leo A, Gomez HL, Aziz Z, Zvirbule Z, Bines J, Arbushites MC *et al.* (2008). Phase III, double-blind, randomized study comparing lapatinib plus paclitaxel with placebo plus paclitaxel as first-line treatment for metastatic breast cancer. *J Clin Oncol* **26**: 5544–5552.

Eichhorn PJ, Gili M, Scaltriti M, Serra V, Guzman M, Nijkamp W *et al.* (2008). Phosphatidylinositol 3-kinase hyperactivation results in lapatinib resistance that is reversed by the mTOR/phosphatidylinositol 3-kinase inhibitor NVP-BEZ235. *Cancer Res* **68**: 9221–9230.

Geyer CE, Forster J, Lindquist D, Chan S, Romieu CG, Pienkowski T *et al.* (2006). Lapatinib plus capecitabine for HER2-positive advanced breast cancer. *N Engl J Med* **355**: 2733–2743.

Gomez HL, Doval DC, Chavez MA, Ang PC, Aziz Z, Nag S *et al.* (2008). Efficacy and safety of lapatinib as first-line therapy for ErbB2-amplified locally advanced or metastatic breast cancer. *J Clin Oncol* **26**: 2999–3005.

Gong Y, Somwar R, Politi K, Balak M, Chmielecki J, Jiang X *et al.* (2007). Induction of BIM is essential for apoptosis triggered by EGFR kinase inhibitors in mutant EGFR-dependent lung adenocarcinomas. *PLoS Med* **4**: e294.

Gymnopoulos M, Elsliger MA, Vogt PK. (2007). Rare cancer-specific mutations in PIK3CA show gain of function. *Proc Natl Acad Sci USA* **104**: 5569–5574.

Hoeflich KP, O'Brien C, Boyd Z, Cavet G, Guerrero S, Jung K *et al.* (2009). *in vivo* antitumor activity of MEK and phosphatidylinositol 3-kinase inhibitors in basal-like breast cancer models. *Clin Cancer Res* **15**: 4649–4664.

Isakoff SJ, Engelman JA, Irie HY, Luo J, Brachmann SM, Pearline RV *et al.* (2005). Breast cancer-associated PIK3CA mutations are oncogenic in mammary epithelial cells. *Cancer Res* **65**: 10992–11000.

Kanwar JR, Shen WP, Kanwar RK, Berg RW, Krissansen GW. (2001). Effects of survivin antagonists on growth of established tumors and B7-1 immunogene therapy. *J Natl Cancer Inst* **93**: 1541–1552.

Kataoka Y, Mukohara T, Shimada H, Saijo N, Hirai M, Minami H. (2010). Association between gain-of-function mutations in PIK3CA and resistance to HER2-targeted agents in HER2-amplified breast cancer cell lines. *Ann Oncol* **21**: 255–262.

Konecny GE, Pegram MD, Venkatesan N, Finn R, Yang G, Rahmeh M *et al.* (2006). Activity of the dual kinase inhibitor lapatinib (GW572016) against HER-2-overexpressing and trastuzumab-treated breast cancer cells. *Cancer Res* **66**: 1630–1639.

LoRusso PM, Jones SF, Koch KM, Arya N, Fleming RA, Loftiss J *et al.* (2008). Phase I and pharmacokinetic study of lapatinib and docetaxel in patients with advanced cancer. *J Clin Oncol* **26**: 3051–3056.

McKenzie JA, Liu T, Goodson AG, Grossman D.. (2010). Survivin enhances motility of melanoma cells by supporting Akt activation and {alpha}5 inte. *Cancer Res* **70**: 7927–7937.

Olie RA, Simoes-Wust AP, Baumann B, Leech SH, Fabbro D, Stahel RA *et al.* (2000). A novel antisense oligonucleotide targeting survivin expression induces apoptosis and sensitizes lung cancer cells to chemotherapy. *Cancer Res* **60**: 2805–2809.

Peirce SK, Findley HW, Prince C, Dasgupta A, Cooper T, Durden DL.. (2010). The PI-3 kinase-Akt-MDM2-survivin signaling axis in high-risk neuroblastoma: a target for PI-3 kinase inhibitor intervention. *Cancer Chemother Pharmacol*: DOI 10.1007/s00280-1010-1486-7.

Saal LH, Holm K, Maurer M, Memeo L, Su T, Wang X *et al.* (2005). PIK3CA mutations correlate with hormone receptors, node metastasis, and ERBB2, and are mutually exclusive with PTEN loss in human breast carcinoma. *Cancer Res* **65**: 2554–2559.

Samuels Y, Wang Z, Bardelli A, Silliman N, Ptak J, Szabo S *et al.* (2004). High frequency of mutations of the PIK3CA gene in human cancers. *Science* **304**: 554.

Serra V, Markman B, Scaltriti M, Eichhorn PJ, Valero V, Guzman M *et al.* (2008). NVP-BEZ235, a dual PI3K/mTOR inhibitor, prevents PI3K signaling and inhibits the growth of cancer cells with activating PI3K mutations. *Cancer Res* **68**: 8022–8030.

Slamon DJ. (1990). Studies of the HER-2/neu proto-oncogene in human breast cancer. *Cancer Invest* **8**: 253.

Slamon DJ, Clark GM, Wong SG, Levin WJ, Ullrich A, McGuire WL. (1987). Human breast cancer: correlation of relapse and survival with amplification of the HER-2/neu oncogene. *Science* **235**: 177–182.

Slamon DJ, Godolphin W, Jones LA, Holt JA, Wong SG, Keith DE *et al.* (1989). Studies of the HER-2/neu proto-oncogene in human breast and ovarian cancer. *Science* **244**: 707–712.

Speliotes EK, Uren A, Vaux D, Horvitz HR. (2000). The survivin-like C. elegans BIR-1 protein acts with the Aurora-like kinase AIR-2 to affect chromosomes and the spindle midzone. *Mol Cell* **6**: 211–223.

Stemke-Hale K, Gonzalez-Angulo AM, Lluch A, Neve RM, Kuo WL, Davies M *et al.* (2008). An integrative genomic and proteomic analysis of PIK3CA, PTEN, and AKT mutations in breast cancer. *Cancer Res* **68**: 6084–6091.

Tanaka K, Iwamoto S, Gon G, Nohara T, Iwamoto M, Tanigawa N. (2000). Expression of survivin and its relationship to loss of apoptosis in breast carcinomas. *Clin Cancer Res* **6**: 127–134.

Toi M, Iwata H, Fujiwara Y, Ito Y, Nakamura S, Tokuda Y *et al.* (2009). Lapatinib monotherapy in patients with relapsed, advanced, or metastatic breast cancer: efficacy, safety, and biomarker results from Japanese patients phase II studies. *Br J Cancer* **101**: 1676–1682.

Uren AG, Wong L, Pakusch M, Fowler KJ, Burrows FJ, Vaux DL *et al.* (2000). Survivin and the inner centromere protein INCENP show similar cell-cycle localization and gene knockout phenotype. *Curr Biol* **10**: 1319–1328.

Zhang H, Liu G, Dziubinski M, Yang Z, Ethier SP, Wu G. (2008). Comprehensive analysis of oncogenic effects of PIK3CA mutations in human mammary epithelial cells. *Breast Cancer Res Treat* **112**: 217–227.

Zhao JJ, Liu Z, Wang L, Shin E, Loda MF, Roberts TM. (2005). The oncogenic properties of mutant p110alpha and p110beta phosphatidylinositol 3-kinases in human mammary epithelial cells. *Proc Natl Acad Sci USA* **102**: 18443–18448.

Supplementary Information accompanies the paper on the Oncogene website (http://www.nature.com/onc)

Clinical Effectiveness of Boron Neutron Capture Therapy for a Recurrent Malignant Peripheral Nerve Sheath Tumor in the Mediastinum

Masayoshi Inoue, MD, PhD, Chun Man Lee, MD, PhD,† Koji Ono, MD, PhD,‡ Minoru Suzuki, MD, PhD,‡ Toshiteru Tokunaga, MD,* Yoshiki Sawa, MD, PhD,† and Meinoshin Okumura, MD, PhD**

A 70-year-old woman underwent extirpation of a malignant peripheral nerve sheath tumor, 4.5 × 2.0 cm in size, in the right supraclavicular fossa. Locoregional recurrence was found 10 months after operation (Figure 1). Although one course of systemic chemotherapy using cisplatin (80 mg/m^2 at day 1) and vinorelbine (25 mg/m^2 at days 1 and 8) was given, the recurrent tumor progressed. Because conventional radiotherapy is not effective for malignant peripheral nerve sheath tumor, boron neutron capture therapy (BNCT) was considered based on the subcutaneous mediastinal location. After institutional review board approval and securing the patient's written informed consent, accumulation of p-boronophenylalanine (BPA) in the tumor was confirmed using 18F-BPA positron emission tomography. Using simulation environment for radiation applications software program, fast neutron and γ-ray physical doses, compound biologic effectiveness- and relative biologic effectiveness-weighted doses, were calculated.

The patient underwent two courses of BNCT with an interval of 3 weeks. BPA-fructose was administered intravenously at a dose of 500 mg/kg just before irradiation. For the first course, the epithermal neutron irradiation was performed for 105 minutes. The dose distribution in the tumor ranged from 13.7 to 22.3 Gy-Eq and was 6.0 Gy-Eq to the skin. For the second course, the irradiation time was shortened to 51 minutes, because of the higher epithermal neutron flux. The dose delivered to the tumor ranged from 6.0 to 24.3 Gy-Eq and was 9.7 Gy-Eq to the skin.

Chest computed tomography scan 1 year after BNCT showed that the tumor size decreased from 6.2 × 4.0 cm to 4.6 × 3.2 cm in size (25% reduction), and stable disease was maintained for 24 months (Figure 2). Positron emission tomography-computed tomography 18 months after BNCT showed no uptake of 18F-fluorodeoxy glucose in the residual mass, suggesting no viability (Figure 3). Neuralgia of the right arm improved. Although temporary dysphagia because of an oral mucosa disorder was observed as a side effect, the patient's general quality of life was preserved. There is no evidence of recurrence 2 years after BNCT.

DISCUSSION

When ^{10}Boron absorbs thermal neutrons, α and ^{7}Lithium particles are generated.[1] BNCT selectively injures the tumor cells containing ^{10}Boron; it was suitable in this case with tumor invasion into the neighboring great vessels. Because the peak of thermal neutron flux is 3 cm beneath the tissue surface, its clinical applications have been limited to malignant melanomas and brain tumors. Kato et al.[2] reported its efficacy for head and neck malignancies. The indication was extended to metastatic liver tumor,[3] malignant mesothelioma,[4] and glioblastoma.[5] This is the first case of mediastinal tumor treated with BNCT.

The effect of BNCT is critically dependent on selective accumulation of ^{10}Boron compounds. The tumor/normal tissue ratio of the ^{10}Boron uptake was 2 in this case, while a ratio greater than 2.5 is preferable for selective treatment. BNCT might be a treatment option for subcutaneous mediastinal tumors, which is resistant to conventional irradiation.

REFERENCES

1. Barth RF, Coderre JA, Vicente MG, et al. Boron neutron capture therapy of cancer: current status and future prospects. *Clin Cancer Res* 2005; 11:3987–4002.
2. Kato I, Ono K, Sakurai Y, et al. Effectiveness of BNCT for recurrent head and neck malignancies. *Appl Radiat Isot* 2004;61:1069–1073.
3. Wittig A, Malago M, Collette L, et al. Uptake of two 10B-compounds in liver metastases of colorectal adenocarcinoma for extracorporeal irradiation with boron neutron capture therapy (EORTC Trial 11001). *Int J Cancer* 2008;122:1164–1171.
4. Suzuki M, Sakurai Y, Masunaga S, et al. Feasibility of boron neutron capture therapy (BNCT) for malignant pleural mesothelioma from a viewpoint of dose distribution analysis. *Int J Radiat Oncol Biol Phys* 2006;66:1584–1589.
5. Vos MJ, Turowski B, Zanella FE, et al. Radiologic findings in patients treated with boron neutron capture therapy for glioblastoma multiforme within EORTC trial 11961. *Int J Radiat Oncol Biol Phys* 2005;61:392–399.

*Department of General Thoracic Surgery, Osaka University Graduate School of Medicine, Suita, Osaka; †Medical Center for Translational Research, Osaka University Hospital, Suita, Osaka; and ‡Radiation Oncology Research Laboratory, Research Reactor Institute, Kyoto University, Kyoto, Japan.

Disclosure: The authors declare no conflicts of interest.

Address for correspondence: Meinoshin Okumura, MD, Department of General Thoracic Surgery, Osaka University Graduate School of Medicine, L5-2-2 Yamadaoka, Suita, Osaka 565-0781, Japan. E-mail: meinosin@thoracic.med.osaka-u.ac.jp

ISSN: 1556-0864/10/0512-2037

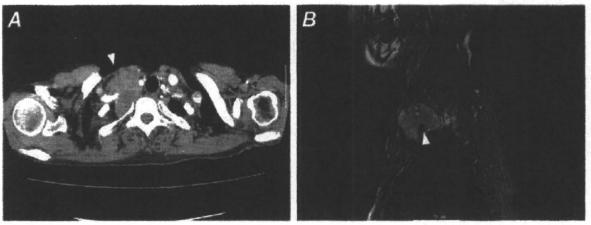

FIGURE 1. Chest computed tomography (CT) scan and magnetic resonance imaging (MRI) showing the recurrent lesion. *A*, Postoperative recurrence, 4.5 × 2.0 cm in size, is seen in the right subclavicular region (arrow head) in the follow-up CT scan 10 months after operation. *B*, Tumor invasion into the right subclavicular artery and brachiocephalic vein is seen (arrow head) in the sagittal view of MRI.

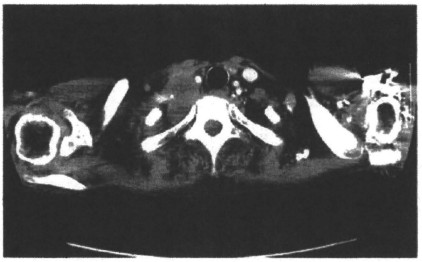

FIGURE 2. Chest computed tomography scan 1 year after boron neutron capture therapy shows shrinkage of the recurrent lesion after chemotherapy from 6.2 × 4.0 cm to 4.6 × 3.2 cm in size (25% reduction).

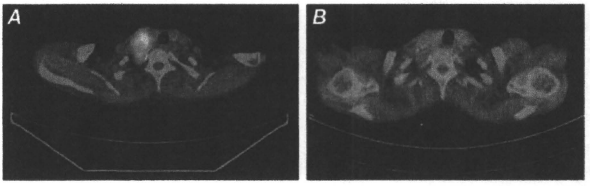

FIGURE 3. FDG-positron emission tomography (PET) shows the remarkable effect of boron neutron capture therapy (BNCT). *A*, PET-computed tomography (CT) before BNCT shows significant tumor uptake. *B*, Although a residual mass is seen, the FDG uptake is reduced to the background level 18 months after BNCT.

ELSEVIER

European Journal of Cardio-thoracic Surgery xxx (2011) xxx–xxx

EUROPEAN JOURNAL OF CARDIO-THORACIC SURGERY

www.elsevier.com/locate/ejcts

Winner of the EACTS Young Investigator Award 2010 - Category 'Thoracic'.

Novel approach for detection of isolated tumor cells in pulmonary vein using negative selection method: morphological classification and clinical implications☆,☆☆

Soichiro Funaki, Noriyoshi Sawabata*, Tomoyuki Nakagiri, Yasushi Shintani, Masayoshi Inoue, Yoshiki Kadota, Masato Minami, Meinoshin Okumura

Department of General Thoracic Surgery, Osaka University Graduate School of Medicine, Osaka, Japan

Received 10 August 2010; received in revised form 28 October 2010; accepted 4 November 2010

Abstract

Objective: The presence of isolated tumor cells (ITCs) in the pulmonary vein (PV) of a lung resected for lung cancer has been reported to be a prognostic factor. Previous investigations noted correlations between prognosis and the presence or amount of ITCs, although few studies have investigated the clinical implications of the morphological characteristics of those cells. We assessed the clinical implications of ITCs in the PV using a novel enrichment approach that maintained their morphological characteristics. **Methods:** Ninety-four consecutive patients with primary non-small-cell lung cancer (NSCLC) without preoperative chemo- and/or radiation therapy (p-stage I in 75, II in 13, III or IV in six) were studied. Blood samples were drawn from the PV draining the lung just after pulmonary resection, and ITCs were enriched using a CD45-negative selection method and density-gradient centrifugation, followed by Papanicolaou staining using 1 ml of PV blood and immunohistochemical staining for cytokeratin in cases with an additional available blood sample. The ITCs were classified into four types based on patterns of cluster formation: no tumor cells (N), singular tumor cells (S), clustered cells ($\leq$0.2 mm) (CSs), and bulky clustered cells (>0.2 mm) (BCSs). We evaluated the correlations between ITC morphology and clinical results. **Results:** ITCs were detected in 68 of 94 patients (72%), of which the BCS type was observed in two, CS in 33, S in 33, and N in 26. Over a median follow-up period of 13 months (range 6–22 months), cancer recurrence occurred in 16 cases (17%): 14 in the combined CS/BCS group, one in S, and one in N. Log-rank analysis revealed that the disease-free survival rate was exclusively worse in patients with clustered ITCs as compared with the other two groups ($p < 0.01$). **Conclusions:** The present method was useful to detect and enrich ITCs from the PV, and showed the clinical relevance of their morphology in lung cancer cases. The presence of ITC clusters may be a prognostic biomarker for patients with resected NSCLC.

Keywords: Lung cancer; Surgery; Isolated tumor cells; Morphology

1. Introduction

Primary lung cancer remains a leading cause of cancer death in most industrialized countries [1], with most cancer deaths related to high rates of recurrence and distant metastasis; thus, useful biomarkers are needed for early detection of both. Recently, isolated tumor cells (ITCs) in blood were reported to be useful markers for prognosis, recurrence, and metastasis [2]. It has been speculated that ITCs are likely shed from the primary tumor, then flow through a drainage vein and circulate throughout the body.

A number of methods to detect ITCs have been reported, with polymerase chain reaction (PCR)-based assays the most widely used [3], as a high sensitivity of ITC detection and clinical implications of the results have been shown [4–6]. Recently, the CellSearch® System (Veridex LLC, Rartian, NJ, USA) was shown to provide accurate detection and enrichment of rare ITCs from blood samples of patients with various types of solid cancer, including lung cancer [7], colon cancer [8], and breast cancer at the single cell level [9]. In addition,

☆ Presented at the 24th Annual Meeting of the European Association for Cardio-thoracic Surgery, Geneva, Switzerland, September 11–15, 2010.

☆☆ This research was supported by a Grant-in-Aid for Scientific Research (B) from the Japan Ministry of Education, Science, Sports and Culture, and the Uehara Memorial Foundation.

* Corresponding author. Address: Department of General Thoracic Surgery, Osaka University Graduate School of Medicine, L-5 2-2 Yamadaoka Suita-city, Osaka, 565-0897, Japan. Tel.: +81 6 6879 3152; fax: +81 6 857 3179.

E-mail addresses: sawabata@thoracic.med.osaka-u.ac.jp, nsawabata@hotmail.com (N. Sawabata).

1010-7940/$ – see front matter
doi:10.1016/j.ejcts.2010.11.029

DOCTOPIC: 9,10,12,15

associations between the number of ITCs with tumor stage and progression have been reported [10]. Most previous studies were quantitative investigations used to evaluate ITCs, and there are few reports of the clinical implication of ITCs that used morphological classification. We conducted the present investigation to assess the clinical implications and morphological characteristics of ITCs in the PV of resected lungs of non-small-cell lung cancer (NSCLC) patients using a novel approach for ITC enrichment and detection.

2. Patients and methods

2.1. Cell-spiking experiment

Initially, to evaluate the accuracy and sensitivity of our method to detect ITCs, a cell-spiking experiment was performed using two lung cancer cell lines, COR-L32 (human small-cell lung carcinoma; ATCC® Catalogue No. 96020744) and SK-LU-1 (human adenocarcinoma; ATCC® Catalogue No. HTB-57™), prior to the examination of clinical samples to detect ITCs in blood samples. The cell lines were maintained in Eagle's Minimum Essential Medium (EMEM) supplemented with fetal bovine serum (FBS) to a final concentration of 10% and incubated at 37 °C. After adding a known number of cells to 1-ml whole blood samples obtained from healthy volunteers, we assessed the sensitivity of our method by determining the ratio of the number of enriched cells to the number of added cells with a hemacytometer.

The method of cell extraction employed was as follows. A RosetteSep® Human CD45 Depletion Cocktail (Stemcell Technologies, Inc.) was added at 50 $\mu l\ ml^{-1}$ to individual whole blood samples and mixed well. After incubation for 20 min at room temperature, the mixture was diluted with an equal volume of phosphate-buffered saline + 2% fetal bovine serum (PBS + 2% FBS) and mixed gently. The diluted sample was then layered on top of a Ficoll-Paque™ PLUS and centrifuged for 20 min at 1200 × g at room temperature, with the brake in the off position; then, the enriched ITCs were removed from the Ficoll-Paque™ PLUS—plasma interface. After washing enriched ITCs with PBS + 2% FBS, the cells were centrifuged down to polylysine-coated glass slides using a cytospin device at 1000 × g for 3 min. Cells on the slides were stained using Papanicolaou stain and a cytokeratin immunohistochemistry kit (Carcinoma cell detection kit human, Miltenyi Biotec® Catalogue No. 130-090-463), which resulted in a cell collection ratio of 60% for both single cells and clustered cells. Tumor cells that existed among the total nuclear cell count ranged from 1×10^2 to 1×10^3 in number.

Table 1. Patient characteristics and distribution of isolated tumor cells in pulmonary venous blood.

	Total	PV cytology			p-Value
		N	S	C	
No.	94	26	33	35	
Gender					0.8
Male	56	17	19	20	
Female	38	9	14	15	
Age (mean ± SD)	67.7 ± 8.4	68.8 ± 8.3	67.2 ± 9.0	70.0 ± 10.9	0.5
<70	49	14	21	14	0.1
≥70	45	12	12	21	
pT factor					0.3
T1	52	18	19	15	
T2	36	7	12	17	
T3	6	1	2	3	
pN factor					1.0
N0	84	24	29	31	
N1	4	1	2	1	
N2	5	1	2	2	
NX	1	0	0	1	
pM factor					1.0
M0	93	26	33	34	
M1a	1	0	0	1	
M1b	0	0	0	0	
p-Stage					0.6
I	75	23	27	25	
II	13	2	4	7	
III or IV	6	1	2	3	
Tumor histology					0.9
Adenocarcinoma	71	19	26	26	
Squamous cell carcinoma	14	4	5	5	
Miscellaneous	9	3	2	4	
Tumor location					0.1
RU	44	13	13	18	
RM	3	0	3	0	
RL	13	2	6	5	
LU	23	4	9	10	
LL	11	7	2	2	

PV, pulmonary vein; N, no tumor cells; S, singular tumor cells; CS/BCS, clustered tumor cells; RU, right upper lobe; RM, right middle lobe; RL, right lower lobe; LU, left upper lobe; LL, left lower lobe.

Please cite this article in press as: Funaki S, et al. Novel approach for detection of isolated tumor cells in pulmonary vein using negative selection method: morphological classification and clinical implications. Eur J Cardiothorac Surg (2010), doi:10.1016/j.ejcts.2010.11.029

2.2. Patients

Ninety-four consecutive patients (56 males, 38 females; range 28–88 years old, median 67.7 years) with primary NSCLC, who did not undergo preoperative chemo- and/or radiation therapy, were evaluated using our method (Table 1). Written informed consent was obtained from all patients enrolled. This study conformed to the ethical guidelines of Osaka University Graduate School of Medicine, and was approved by the institutional review board of Osaka University Medical Hospital. All patients underwent a segmentectomy ($n = 11$), lobectomy ($n = 80$), or bilobectomy ($n = 3$) with a systematic mediastinal lymphadenectomy from August 2008 to January 2010 at Osaka University Medical Hospital.

The postoperative staging of all patients was determined according to the tumor–node–metastasis (TNM) classification of the Union for International Cancer Control (UICC), ver. 7, 2009 (Table 1). The median follow-up duration was 13 months (6–22 months). In follow-up examinations, all patients were evaluated at 3-month intervals. Each evaluation included a physical examination, chest X-ray, and blood tests including tumor markers, while additional thoracic–abdominal computed tomography (CT) scans were generally performed at 6-month intervals.

2.3. Blood samples and ITC detection and enrichment

All blood samples were collected on the back table immediately after lung resection by gentle aspiration with an 18-gauge needle from the tumor-draining pulmonary vein (PV), which was stapled before the resection in all cases, and placed in 10-ml ethylene diamine tetraacetic acid (EDTA) tubes. ITCs were isolated using a negative selection method from 1-ml blood samples by the method described above. In addition, cytokeratin immunohistochemistry was performed, if an additional blood sample was available.

2.4. Evaluation and classification of clusters

Using all of the samples, one glass slide containing enriched ITCs from each patient was prepared and assessed by Papanicolaou staining. This examination was performed independently by two cytologists (E.Y and H.Y) who were unaware of the patient's clinical data. For morphological assessment, each cytologist distinguished cancer cells from normal cells by light microscopy based on their morphological appearance, such as cell size and shape, nuclear size and shape, and nuclear–cytoplasmic ratio (N/C). Furthermore, for cluster formation assessment, patterns of ITCs were classified into the following four types: no tumor cells (N), singular cells (S), clustered cells ($\leq$0.2 mm in size) (CSs) including singular cells, and bulky clustered cells (>0.2 mm in size) (BCSs), which included clustered cells and singular cells.

2.5. Statistical analysis

Statistical analysis was performed using the SPSS Exact Tests software. The Kruskal–Wallis test was used to calculate mean values, and prevalence was analyzed with Fisher's exact test. For analysis of follow-up data, survival curves were calculated with the Kaplan–Meier method and survival distributions were compared by a log-rank test. The Cox proportional hazards model was applied for calculating hazard ratio by uni- and multivariate analyses. The threshold for statistical significance was a p-value less than 0.05.

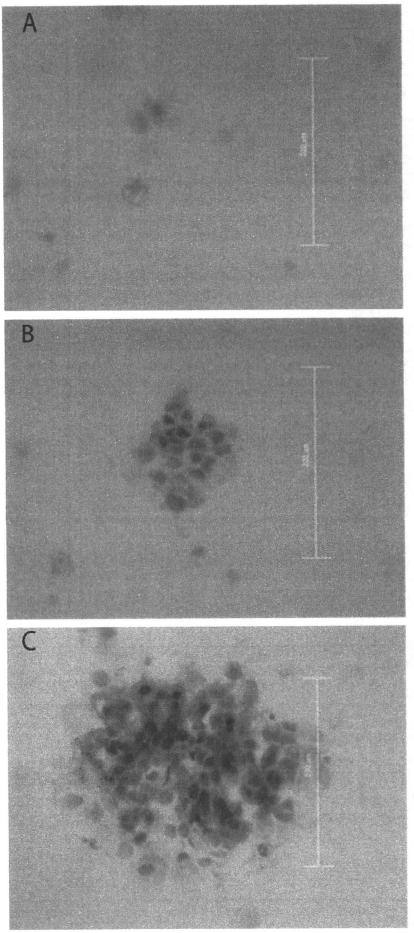

Fig. 1. Classification of isolated tumor cells by cluster formation. Shown are results following Papanicolaou staining. (A) Arrows indicate singular cancer cells. (B) Clustered cancer cells ($\leq$0.2 mm). (C) Bulky clustered cells (>0.2 mm). Original magnification ×40. Scale bars = 0.2 mm.

Please cite this article in press as: Funaki S, et al. Novel approach for detection of isolated tumor cells in pulmonary vein using negative selection method: morphological classification and clinical implications. Eur J Cardiothorac Surg (2010), doi:10.1016/j.ejcts.2010.11.029

3. Results

3.1. Detection of ITCs

Using Papanicolaou staining, ITCs classified as S were detected in 33 (35%) of the 94 patients, while those classified as CS or BCS were found in 35 (37%). Fig. 1 shows examples of singular and cluster formations of CTCs. Cases classified as CS and BCS were considered as a single group for analysis of survival, as the number of BCS cases was small. Cytokeratin examinations were performed in 59 cases (15 classified as N, 21 as S, 22 as CS, and one as BCS). All cases classified as CS or BCS revealed positive results for cytokeratin staining, whereas only seven (33%) of those classified as S and none as N showed positive cytokeratin staining results.

3.2. ITC classification and prognosis

The correlations of patient characteristics with distribution of ITCs in pulmonary venous blood are shown in Table 1. There were no significant differences regarding patient characteristics among the three groups (N, S, and CS/BCS). Sixteen patients suffered cancer relapse, including 14 in the CS/BCS group, one in S, and one in N: these could be detailed as exclusive local recurrence in four (pleura in one, chest wall in one, hilar lymph node in one, mediastinal lymph node in one), local and distant metastasis in seven (bilateral lungs in four, mediastinal lymph node and neck lymph node in two, mediastinal lymph node and bone in one), and exclusive distant metastasis in five (contralateral lung in three, adrenal gland in one, and brain and liver in one). Relapse-free survival curves are shown in Fig. 2, which demonstrated that the cluster group (CS/BCS) exclusively was statistically significant; overall survival curves are shown in Fig. 3. Univariate analysis revealed that the presence of clustered ITCs and p-stage III or IV were significant prognostic factors in the analysis of disease-free survival, and those results were confirmed by multivariate analysis findings (Table 2).

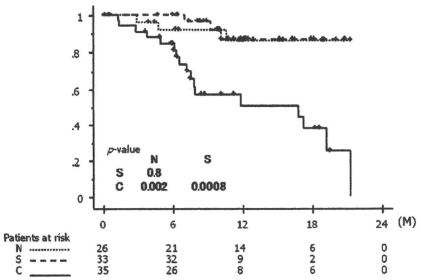

Fig. 2. Relapse-free survival curves.
N, patients with no tumor cells; S, patients with singular tumor cells; C, patients with clustered tumor cells (CS/BCS).

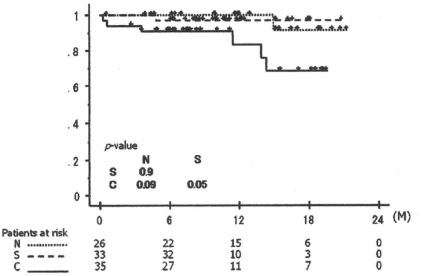

Fig. 3. Overall survival curves.
N, patients with no tumor cells; S, patients with singular tumor cells; C, patients with clustered tumor cells (CS/BCS).

4. Discussion

In the present study, we focused on the morphological appearance of ITCs and investigated related clinical implications. Our results showed that cluster formations of ITCs may be a prognostic indicator for early recurrence of lung cancer. In cases with singular cancer cells, the recurrence rate was low as compared with those with cluster formation. However, the clinical implications of the presence of singular ITCs remain unclear and a longer duration follow-up study is needed to determine clinical outcomes over a long period.

In spite of early discovery of cancer and complete surgical resection, the rates of recurrence and mortality in lung cancer cases remain high [1]. During treatment of postoperative patients, it is especially important to detect early relapse and distant metastasis. Thus, it is crucial to develop useful biomarkers for predicting early recurrence and metastasis. Some recent studies have demonstrated that the presence of ITCs in circulating blood was useful as a biomarker for the prognosis of various types of disease, such as breast cancer [7], colorectal cancer [6], and lung cancer [11].

Various methods to detect and enrich ITCs have been reported. In older studies, ITCs were observed using whole blood samples [12], though those results are not considered to be reliable. Recently, Sienel et al. used a cytokeratin immunohistochemistry method to reveal that the presence of ITCs in samples collected from the PV of a pulmonary lobe containing lung cancer before resection was a predictor of poor survival [13]. In addition, Yamashita et al. reported a study that used reverse transcriptase-polymerase chain reaction (RT-PCR) assays of peripheral blood to detect messenger RNA (mRNA) of carcinoembryonic antigen (CEA), and noted that its presence was a prognostic indicator in patients with NSCLC [11]. Current advancement in technology allow for ITCs to be captured and quantitatively evaluated with the semi-automated CellSearch® System (Veridex LLC, NJ, USA). Using this system, some groups have reported that determination of the number of pre- and postoperative ITCs was useful as a biomarker for survival and prognosis [7,10], while another showed that those results were able to reveal cancer cell spreading caused by the operation [14]. However, most of those studies used

Please cite this article in press as: Funaki S, et al. Novel approach for detection of isolated tumor cells in pulmonary vein using negative selection method: morphological classification and clinical implications. Eur J Cardiothorac Surg (2010), doi:10.1016/j.ejcts.2010.11.029

Table 2. Results of univariate and multivariate analyses of relapse-free survival.

Variables	Univariate			Multivariate		
	R.R.	95% C.I.	p-Value	R.R.	95% C.I.	p-Value
ITCs in PV						
None	Ref.			Ref.		
Singular	0.901	0.180–4.505	0.9	0.845	0.170–4.577	0.9
Clustered	5.894	1.717–20.23	0.005	8.882	1.676–21.04	0.006
Gender						
Male	Ref.					
Female	0.882	0.355–1.904	0.7	0.895	0.319–2.515	0.8
Age in years						
<70	Ref.					
≥70	1.923	0.831–4.446	0.1	1.279	0.490–3.339	0.6
p-Stage						
I	Ref.					
II	2.122	0.686–6.557	0.2	2.096	0.588–7.474	0.3
III or IV	7.591	2.612–22.06	0.0002	9.756	3.357–40.37	0.002
Tumor histology						
Adenocarcinoma	Ref.					
Squamous cell carcinoma	1.717	0.560–5.265	0.3	2.147	0.588–7.847	0.2
Miscellaneous	2.456	0.806–7.482	0.1	1.081	0.225–5.204	0.9

quantitative evaluation methods and few have shown the significance of qualitative evaluation of ITCs.

In the present study, early relapse was associated with the presence of clustered cancer cells. We speculated that cancer cells may be able to live for a longer period in circulating blood when clustered, thus allowing direct access to distant organs and easy establishment of a secondary tumor. In addition, when considering tumor-initiating cells, it is possible that cells with a large diameter have a greater potential of causing relapse [15].

A recent study noted that epithelial–mesenchymal transition (EMT) plays important roles in cancer progression and metastasis [16]. Through the EMT process, the morphology and gene expression of the epithelial markers E-cadherin and cytokeratin become altered in cancer cells [17,18]. Our present analysis using immunohistochemical staining for cytokeratin showed that the positive rate of CS/BCS cases was 100%, whereas that in cases classified as S was low (33%). The reason for the different rates of positivity between S and CS/BCS cases may be related to EMT. Furthermore, the low occurrence of cytokeratin staining in cases classified as S may indicate that the expression of cytokeratin was reduced during the EMT process.

There are some limitations to our method, as accurate cell counting and ITC enrichment have not been perfected. On the other hand, with the CellSearch® system [7–10], cell-number counting and enrichment are easily performed in a semiautomatic fashion, though it is difficult to detect morphological features, in contrast to the method used in the present study. Moreover, there are problems with the procedure used to collect the samples. In the present method, in patients, after resecting the lung and placing it on the back table, blood was collected by aspiration from the PV, which had been stapled before the resection. Ideally, blood samples should be collected from the PV with proximal clamping before lung resection. In addition, it would be good to perform the assays with blood samples obtained from the peripheral vein. Some studies have presented preoperative and postoperative analyses of ITCs obtained from peripheral blood samples [7,11]. In the future, we intend to collect blood samples before lung resection and perform the assays using peripheral blood samples. In addition, we hope to conduct additional research using blood samples obtained at various time points before, during, and after surgery.

In conclusion, the present CD45-negative selection method was found useful to detect and enrich ITCs from blood samples obtained from the PV of lungs resected for NSCLC. In addition, our results show the clinical relevance of morphological classification of ITCs in NSCLC cases, as the presence of clustered ITCs was a prognostic indicator for patients following surgical resection.

Acknowledgments

The authors thank Professor Katsuyuki Aozasa, Dr Eiichi Morii, and Dr Hideo Yoshimura (Department of Pathology, Osaka University Graduate School of Medicine) for their contributions to the cytological diagnosis.

References

[1] Alberg AJ, Ford JG, Samet JM. American College of Chest Physicians. Epidemiology of lung cancer: ACCP evidence-based clinical practice guidelines (2nd edition). Chest 2007;132:29S–55S.
[2] Pantel K, Brakenhoff RH, Brandt B. Detection, clinical relevance and specific biological properties of disseminating tumour cells. Nat Rev Cancer 2008;8:329–40.
[3] Smith B, Selby P, Southgate J, Pittman K, Bradley C, Blair GE. Detection of melanoma cells in peripheral blood by means of reverse transcriptase and polymerase chain reaction. Lancet 1991;338:1227–9.
[4] Kurusu Y, Yamashita J, Ogawa M. Detection of circulating tumor cells by reverse transcriptase-polymerase chain reaction in patients with resectable non-small-cell lung cancer. Surgery 1999;126:827–8.
[5] Iinuma H, Okinaga K, Egami H, Mimori K, Hayashi N, Nishida K, Adachi M, Mori M, Sasako M. Usefulness and clinical significance of quantitative real-time RT-PCR to detect isolated tumor cells in the peripheral blood and tumor drainage blood of patients with colorectal cancer. Int J Oncol 2006;28:297–306.
[6] Ignatiadis M, Xenidis N, Perraki M, Apostolaki S, Politaki E, Kafousi M, Stathopoulos EN, Stathopoulou A, Lianidou E, Chlouverakis G, Sotiriou C, Georgoulias V, Mavroudis D. Different prognostic value of cytokeratin 19 mRNA positive circulating tumor cells according to estrogen receptor and HER2 status in early-stage breast cancer. J Clin Oncol 2007;25:5194–202.
[7] Okumura Y, Tanaka F, Yoneda K, Hashimoto M, Takuwa T, Kondo N, Hasegawa S. Circulating tumor cells in pulmonary venous blood of primary lung cancer patients. Ann Thorac Surg 2009;87:1669–75.

Please cite this article in press as: Funaki S, et al. Novel approach for detection of isolated tumor cells in pulmonary vein using negative selection method: morphological classification and clinical implications. Eur J Cardiothorac Surg (2010), doi:10.1016/j.ejcts.2010.11.029

[8] Sastre J, Maestro ML, Puente J, Veganzones S, Alfonso R, Rafael S, Garcia-Saenz JA, Vidaurreta M, Martin M, Arroyo M, Sanz-Casla MT, Diaz-Rubio E. Circulating tumor cells in colorectal cancer: correlation with clinical and pathological variables. Ann Oncol 2008;19:935–8.
[9] Cristofanilli M, Budd GT, Ellis MJ, Stopeck A, Matera J, Miller MC, Reuben JM, Doyle GV, Allard WJ, Terstappen LW, Hayes DF. Circulating tumor cells, disease progression, and survival in metastatic breast cancer. N Engl J Med 2004;351:781–91.
[10] Tanaka F, Yoneda K, Kondo N, Hashimoto M, Takuwa T, Matsumoto S, Okumura Y, Rahman S, Tsubota N, Tsujimura T, Kuribayashi K, Fukuoka K, Nakano T, Hasegawa S. Circulating tumor cell as a diagnostic marker in primary lung cancer. Clin Cancer Res 2009;15:6980–6.
[11] Yamashita J, Matsuo A, Kurusu Y, Saishoji T, Hayashi N, Ogawa M. Preoperative evidence of circulating tumor cells by means of reverse transcriptase-polymerase chain reaction for carcinoembryonic antigen messenger RNA is an independent predictor of survival in non-small cell lung cancer: a prospective study. J Thorac Cardiovasc Surg 2002;124:299–305.
[12] Stuart R, Alvin W, Ruth M, Elizabeth M, Warren C. Technique and results of isolation of cancer cells from the circulating blood. AMA Arch of Surg 1958;76:334–46.
[13] Sienel W, Seen-Hibler R, Mutschler W, Pantel K, Passlick B. Tumour cells in the tumour draining vein of patients with non-small cell lung cancer: detection rate and clinical significance. Eur J Cardiothorac Surg 2003;23:451–6.
[14] Sawabata N, Okumura M, Utsumi T, Inoue M, Shiono H, Minami M, Nishida T, Sawa Y. Circulating tumor cells in peripheral blood caused by surgical manipulation of non-small-cell lung cancer: pilot study using an immunocytology method. Gen Thorac Cardiovasc Surg 2007;55:189–92.
[15] Liotta LA, Kleinerman J, Saidel GM. Quantitative relationships of intravascular tumor cells, tumor vessels, and pulmonary metastases following tumor implantation. Cancer Res 1974;34:997–1004.
[16] Thiery JP, Acloque H, Huang RY, Nieto MA. Epithelial-mesenchymal transitions in development and disease. Cell 2009;139:871–90.
[17] Tsuji T, Ibaragi S, Hu GF. Epithelial-mesenchymal transition and cell cooperativity in metastasis. Cancer Res 2009;69:7135–9.
[18] Koo V, El Mekabaty A, Hamilton P, Maxwell P, Sharaf O, Diamond J, Watson J, Williamson K. Novel in vitro assays for the characterization of EMT in tumourigenesis. Cell Oncol 2010;32:67–76.

Appendix A. Conference discussion

Dr G. Varela (Salamanca, Spain): To my knowledge, you are the first to demonstrate that the presence of clusters of tumor cells in pulmonary venous blood adversely influences the prognosis in pathological stage I non-small cell lung cancer cases.

Previously, different authors have reported the finding of epithelial cells in blood obtained from pulmonary veins after lung resection by means of antibodies against the epithelial cell adhesion molecule using the so-called Cell Search System. According to Passlick, this happens in less than 20% of the resected cases, while Okumura and co-workers reported circulating tumor cells in more than 95% of their cases. With your technique you have detected clusters of tumor cells in around 30% of your cases. This seems to be more specific for tumor cell detection and also more sensitive than simple immunohistochemical staining. I'm wondering if this 30% prevalence of clusters of cells may be related to anatomical conditions or to the type of surgical techniques; for instance, the tumor size or location in the lobe, the way of handling the tumor during surgery, the sequence of vessel ligation and so on.

My second question is, if the finding of clusters of cells is not related to surgical manipulation, maybe comparable findings could be elicited in sequentially-taken samples of peripheral arterial blood prior to surgery, indicating the need for induction chemotherapy even in selected clinical stage IA cases. Do you have any preliminary data on this or are you thinking about a similar study?

Dr Funaki: As you mentioned, I think surgical manipulation is an important problem. I think surgical manipulation may enhance the cancer cells shedding into the bloodstream, as you mentioned, but I don't think that all cancer cells are shed into the bloodstream only by surgical manipulation.

As for the surgical techniques, in our research we first ligate the pulmonary vein. So there is the possibility that surgical manipulation may enhance cancer cells shedding in the bloodstream and that the number of isolated tumor cells may increase.

Please cite this article in press as: Funaki S, et al. Novel approach for detection of isolated tumor cells in pulmonary vein using negative selection method: morphological classification and clinical implications. Eur J Cardiothorac Surg (2010), doi:10.1016/j.ejcts.2010.11.029

ELSEVIER

European Journal of Cardio-thoracic Surgery 37 (2010) 1445–1449

EUROPEAN JOURNAL OF CARDIO-THORACIC SURGERY

www.elsevier.com/locate/ejcts

Clinical outcome of resected solid-type small-sized c-stage IA non-small cell lung cancer

Masayoshi Inoue *, Masato Minami, Noriyoshi Sawabata, Tomoki Utsumi, Yoshihisa Kadota, Norihisa Shigemura, Meinoshin Okumura

Department of General Thoracic Surgery, Osaka University Graduate School of Medicine, 2-2-L5, Yamadaoka, Suita-city, Osaka, 565-0871, Japan

Received 13 September 2009; received in revised form 16 December 2009; accepted 16 December 2009

Abstract

Background: The chances of pulmonary resection for small-sized lung cancer have increased because of the development of thin-slice computed tomography (CT). Though sublobar resection could be indicated for ground glass opacity (GGO)-dominant adenocarcinoma with low-grade behaviour, the malignant potential of solid-type, small-sized lung cancer has not been sufficiently assessed. We aimed to address the clinical outcomes of resected solid-type c-stage IA non-small cell lung cancer (NSCLC) smaller than 2 cm. **Methods:** A retrospective observational study involving 118 patients who had undergone a complete resection for lung cancer smaller than 2 cm with solid component more than 50% on CT was conducted, and their postoperative survival and recurrence pattern were analysed. **Results:** Thirty-five patients with solid component-dominant lesion (SCDL) and 83 patients with pure solid lesion (PSL) without GGO were enrolled. Lymph node involvement was found in 15 patients with PSL (18%). The 5-year disease-free survival (DFS) was 100% in SDCL patients and 83% in PSL patients. Multivariate analysis of PSL patients showed that lymph node metastasis and pleural invasion were independent negative prognostic predictors. The 5-year DFS was 88%, 80% and 46% in p-N0, p-N1 and p-N2 patients, respectively. The 5-year DFS was 33% for patients with pleural invasion, which was significantly worse than that for patients without pleural involvement. Postoperative recurrence was mainly observed as intrathoracic lesions within 3 years. **Conclusions:** A proportion of solid-type NSCLC has malignant potential, even for tumours smaller than 2 cm. Periodic intrathoracic evaluation is required following complete resection.

Keywords: Lung cancer; Surgery; Outcomes; Survival analysis

1. Introduction

Lung cancer is a leading cause of death from cancer. Several clinical trials with multimodal therapy, including adjuvant chemotherapy, have been conducted to improve the outcome of advanced disease, while the efficacy of induction therapy is still controversial [1–4]. Diagnostic imaging such as computed tomography (CT), magnetic resonance imaging (MRI) and positron-emission tomography CT (PET–CT) is now widely available clinically. The recent development of thin-slice and high-resolution CT or low-dose CT screening has particularly increased the chance of treating small-sized lung cancer.

Bronchioloalveolar adenocarcinoma, which is usually detected as ground glass opacity (GGO) on CT imaging, has been identified as a different type of non-small-cell lung cancer (NSCLC) with low-grade malignancy [5]. It has been reported that sublobar resection, such as segmentectomy or wide-wedge resection, is feasible for GGO-dominant lesions [6], while a lobectomy is still a standard procedure for NSCLC. A clinical trial of randomised lobectomy versus sublobar resection for peripheral small-sized lung cancer is ongoing in the USA (CALGB 140503), and a similar trial has been proposed by the Japan Clinical Oncology Group.

However, patients with small-sized NSCLC occasionally have locally advanced disease with lymph node metastases [7–9]. Most such cases have a lesion showing a solid component or solid-dominant GGO on preoperative CT imaging. These solid-type lesions could be a different entity among small-sized lung cancer, most of which is early disease.

The present study focussed on c-stage IA patients with solid component-dominant lesion (SCDL) or pure solid lesion (PSL) small-sized NSCLC, especially patients with PSL to clarify postoperative outcomes and consider the optimal surgical procedure. Disease-free survival (DFS) and the relapse pattern during postoperative follow-up were retrospectively analysed.

2. Materials and methods

2.1. Patients

The records of all 188 consecutive patients with c-stage IA peripheral lung cancer smaller than 2 cm, who underwent a

* Corresponding author. Japan. Tel.: +81 6 6879 3152; fax: +81 6 6879 3164.
E-mail address: mi@thoracic.med.osaka-u.ac.jp (M. Inoue).

1010-7940/$ – see front matter
doi:10.1016/j.ejcts.2009.12.030

complete resection between 1992 and 2007 at the Osaka University Hospital, Osaka, Japan, were reviewed. Institutional Review Board at the Osaka University approved this study, and patient consent was waived. Of these, 118 NSCLC patients with a solid or solid component-dominant lesion, in which the GGO area was less than 50% on thin-slice CT (Table 1), were selected. Follow-up of more than 5 years was completed in 100 patients, and the median follow-up time for all patients was 60.8 months. Preoperative diagnosis was performed by chest radiography and CT imaging, as well as biopsy using fibre optic bronchoscopy or percutaneous core needle biopsy. Core needle biopsy was performed under CT guidance in our institute. Lymph nodes larger than 1 cm in the short axis on CT were clinically defined as metastasis-positive. An ^{18}-fluorodeoxyglucose positron-emission tomography (FDG-PET) and PET–CT were also available for nodal staging from 1997 and 2005, respectively. Mediastinoscopy was performed in two patients with mediastinal lymph node swelling observed in CT. Brain CT or MRI, abdominal CT and bone scintigraphy were used to detect distant metastases for clinical staging. The preoperative serum carcinoembryonic antigen (CEA) level was measured in 113 patients and included in the survival analysis as a variable. We performed a lobectomy with nodal dissection in principle, while sublobar resection was indicated in high-risk cases. Postoperative staging was performed according to the tumour, node, metastasis (TNM) classification. Pleural invasion was histologically evaluated using haematoxylin–eosin (H–E) staining. There was no parietal pleural invasion and only visceral pleural invasion was observed in this study. Adjuvant chemotherapy was indicated in p-stage II and III patients with good status since 2005, and as a result, given in nine patients. One patient had postoperative radiation. Chest and abdominal CT scan, brain CT or MRI and bone scintigraphy were used for postoperative follow-up. Initial recurrence sites and the pattern following complete resection were also evaluated. Variables used for evaluation were age, sex, tumour diameter, operative procedure, histology, serum CEA level, lymph node metastasis and pleural invasion.

Table 1
Characteristics of 118 patients with c-stage IA solid-type non-small cell lung cancer smaller than 2 cm in diameter.

Age (years)	38–83 (median 65)
Sex	
Female	77
Male	41
Tumour diameter (mm)	3–20 (median 15)
Diagnostic method	
Intra-operative rapid section	49
Percutaneous core needle biopsy	39
Transbronchial biopsy	28
Sputum cytology	2
CT finding	
Solid lesion	83
Solid component-dominant lesion	35
Operative procedure	
Lobectomy	90
Segmentectomy	23
Wedge resection	5
Histology	
Adenocarcinoma	97
Squamous cell carcinoma	19
Others	2
p-Stage	
IA	101
IB	2
IIA	4
IIB	1
IIIA	10
Lymph node metastasis*	
p-N1	5
p-N2	10

* The tumors of all patients with nodal metastasis showed pure solid lesion on CT.

2.2. Statistical analyses

DFS and overall survival (OS) were calculated using the Kaplan–Meier method, and the prognostic effects of variables on DFS and OS were analysed using the log rank test and a Cox regression model [10,11].

3. Results

The results of postoperative pathological examination are shown in Table 1. Adenocarcinoma is dominant in this category of solid-type, small-sized NSCLC in our institute. Of the 118 patients, 101 (86%) had accurate clinical staging, though the remaining 14% were underestimated. Hilar and mediastinal lymph node metastases were found in 15 patients (13%) with PSL or SCDL NSCLC smaller than 2 cm. The primary tumour showed pure solid attenuation on CT in these patients with nodal involvement, and 15 (18%) of 83 patients with PSL smaller than 2 cm had lymph node metastases.

The 5-year DFS was 100% for c-stage IA patients with SCDL and 83% for c-stage IA patients with PSL (Fig. 1). Postoperative relapses were observed within 3 years after surgery except in one case, who had recurrence at the resected margin after segmentectomy 10 years after surgery. The 5-year OS was 100% for patients with SCDL and 87% for patients with PSL. Since no recurrence was found and the outcome was excellent in patients with SCDL in the present study, we focussed on the patients with PSL for further analyses.

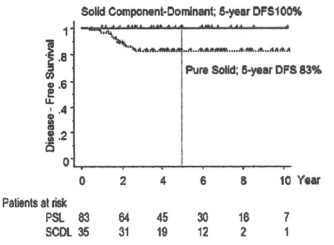

Fig. 1. Disease-free survival (DFS) for c-stage IA patients with solid-type, small-sized, NSCLC who underwent a complete resection. The 5-year DFS is 100% for c-stage IA patients with SCDL and 83% for c-stage IA patients with PSL. SCDL, solid component-dominant lesion; PSL, pure solid lesion.

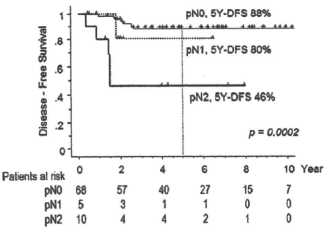

Fig. 2. Disease-free survival (DFS) for c-stage IA patients with pure solid, small-sized tumour by histological lymph node status. The 5-year DFS for patients with p-N0, p-N1, and p-N2 was 88%, 80%, and 46%, respectively.

Patients with PSL underwent a lobectomy in 63, segmentectomy in 17 and wedge resection in three cases. By analysing patients with PSL by pathological lymph node status, the 5-year DFS was 88% for patients with p-N0, 80% for patients with p-N1 and 46% for patients with p-N2 (Fig. 2). The postoperative outcome of patients with node metastases was worse than that for p-N0 patients ($p = 0.0002$). Similar results were obtained in the overall analysis, and the 5-year OS was 95% for p-N0 patients, 50% for p-N1 patients and 56% for p-N2 patients ($p = 0.0009$). Lymph node involvement was a significant prognostic factor for postoperative recurrence and survival in patients with pure solid, small-sized, lung cancer. The distribution of metastatic lymph node by the tumour location was upper + hilar/interlober/peripheral zones for eight tumours in the right upper lobe, upper + -AP + hilar/peripheral zones for three tumours in the left upper lobe and upper + subcarinal + lower + hilar/interlober/peripheral zones for four tumours in the right lower lobe.

Survival was also assessed according to histological pleural invasion. The 5-year DFS for PSL patients was 87% with negative pleural invasion and 33% for positive pleural invasion (Fig. 3); the difference in DFS was significant ($p = 0.0002$), and pleural invasion had a clinically negative impact on postoperative recurrence. The overall survival analysis showed that 5-year OS for PSL patients was 91% with negative pleural invasion and 63% with positive pleural invasion ($p = 0.06$). Thus, pleural invasion was a significant prognostic factor for postoperative recurrence.

Elevated preoperative CEA levels (>5 ng ml^{-1}) were observed in three of 33 SCDL patients (9.1%) and in 35 of 80 PSL patients (43.8%) ($p = 0.0001$, chi-square test). Among PSL patients, the 5-year DFS for patients with a high CEA level was 75%, which was slightly worse than that for patients with a normal CEA (88%), though the difference was not significant ($p = 0.13$).

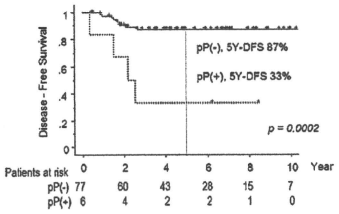

Fig. 3. Disease-free survival (DFS) for c-stage IA patients with pure solid, small-sized tumour by pleural invasion. The 5-year DFS was 87% for patients with negative pleural invasion and 33% for patients with positive pleural invasion.

Univariate analysis using age, sex, tumour size, operative procedure, histology, preoperative CEA level, lymph node metastasis and pleural invasion as the variables revealed that lymph node metastasis was a prognostic factor for both OS and DFS (Table 2) following complete resection of pure solid, small-sized, NSCLC using a proportional hazard model, though pleural invasion was a significant factor only for DFS (Table 2). Multivariate analysis was performed using tumour size and serum CEA level, which was identified to be prognostic factors in small-sized lung cancer in our previous study [12], in addition to lymph node metastasis and pleural invasion

Table 2
Univariate analyses of potential prognostic factors in patients with c-stage IA, pure solid, non-small cell lung cancer smaller than 2 cm.

Variables	Hazard ratio	95% CL	p value
Overall survival			
Age	1.01	0.941–1.09	0.77
Sex			
Female	1		
Male	2.74	0.337–22.5	0.35
Tumour size	1.12	0.913–1.37	0.28
Histology			
Ad	1		
Non-Ad	1.21	0.243–6.01	0.82
Serum CEA level	0.988	0.912–1.07	0.76
LN metastasis			
Negative	1		
Positive	9.14	2.17–38.5	0.003
Pleural invasion			
Negative	1		
Positive	4.11	0.829–20.4	0.084
Operative procedure			
Lobectomy	1		
Sublobar res.	0.522	0.064–4.24	0.54
Disease-free survival			
Age	0.981	0.934–1.03	0.44
Sex			
Female	1		
Male	2.39	0.534–10.7	0.26
Tumour size	1.03	0.898–1.19	0.66
Histology			
Ad	1		
Non-Ad	0.574	0.127–2.59	0.47
Serum CEA level	0.997	0.947–1.05	0.91
LN metastasis			
Negative	1		
Positive	5.81	1.93–17.5	0.002
Pleural invasion			
Negative	1		
Positive	7.04	2.16–22.9	0.001
Operative procedure			
Lobectomy	1		
Sublobar res.	0.900	0.251–3.23	0.87

CL, confidence limit; Ad, adenocarcinoma; LN, lymph node; Sublobar res., sublobar resection (segmentectomy or wedge resection)

Table 3
Multivariate analysis of potential prognostic factors in patients with c-stage IA, pure solid, non-small cell lung cancer smaller than 2 cm.

Variables	Hazard ratio	95% CL	p value
Overall survival			
Tumour size	1.06	0.839–1.34	0.63
Serum CEA level	0.950	0.856–1.06	0.34
LN metastasis			
Negative	1		
Positive	11.0	2.38–51.3	0.002
Pleural invasion			
Negative	1		
Positive	1.87	0.326–10.7	0.48
Disease-free survival			
Tumour size	0.904	0.754–1.08	0.28
Serum CEA level	0.978	0.929–1.03	0.38
LN metastasis			
Negative	1		
Positive	10.2	2.81–37.0	0.0004
Pleural invasion			
Negative	1		
Positive	11.1	2.55–48.6	0.001

CL, confidence limit; LN, lymph node.

showing prognostic tendency or significance with univariate analysis in the present study. There was no significant correlation between lymph node metastasis and pleural invasion in the present study ($p = 0.35$ by chi-square test). While only node involvement significantly influenced overall survival (Table 3), both lymph node metastasis and pleural invasion were detected to be independent risk factors for recurrence (Table 3).

The initial recurrence site was also assessed during postoperative follow-up (Table 4). Of 15 patients, 13 (87%) had intrathoracic relapse, including hilar and mediastinal lymph nodes, pleural dissemination and pulmonary resected margin. The patients suffering relapse at the resected margin included a radical segmentectomy for tumour 1 cm in diameter in the anterior segment of the right upper lobe and a wedge resection for two patients. Distant metastasis was detected in the brain and bone in two patients as an initial relapse site. Two patients had simultaneous recurrence (lymph node + dissemination + lymphangitis, lymph node + pulmonary metastasis). Among 28 patients, who underwent a sublobar resection (23 segmentectomy and five wedge resection), resected margin recurrences were found in three (11%), while no relapse with lymph node metastasis was observed. All three patients suffering resected margin relapse underwent a completion lobectomy and survived for 31, 41 and 138 months without disease.

Table 4
Initial recurrence site on postoperative follow-up.

Recurrence site	Patient number (postoperative months)
Hilar and mediastinal lymph node	8 (11, 17, 18, 19, 21, 22, 22, 30)
Pulmonary resected margin*	3 (25, 25, 127)
Pleural dissemination	2 (12, 18)
Pulmonary metastasis	2 (30, 32)
Lymphangitis carcinomatosa	1 (18)
Brain metastasis	1 (27)
Bone metastasis	1 (5)

Two patients had recurrence in multiple organs.
* All three cases with margin relapse underwent a complete lobectomy.

4. Discussion

Recently, radical sublobar resection, such as a segmentectomy or wide-wedge resection, has been recognised as an option for small-sized lung cancer [13–15], though a lobectomy with nodal dissection is still the gold standard for the treatment of resectable lung cancer [16]. However, patients with locally advanced disease with small-sized primary lesions, which usually show a solid component on CT, are occasionally encountered. Bronchioloalveolar adenocarcinoma showing a pure GGO lesion on CT imaging, which is histopathologically classified as Noguchi A or B type, is well understood to be a low-grade lung cancer [17,18]. A limited resection, such as segmentectomy or wide-wedge resection, could be curative for such slow-growing lung cancers. However, it has been reported that 10–15% of patients with small-sized lesions had nodal involvement [7–9], while we reported the node metastasis ratio as 15% among patients with NSCLC smaller than 2 cm [12]. Thus, we intended to address the characteristics of c-stage IA solid-type NSCLC, which might be also a candidate for sublobar resection, and identified the risk of lymph node metastasis and postoperative local recurrence in patients with a solid tumour. When conducting sublobar resection for such PSL patients, careful preoperative and intra-operative assessments for nodal metastasis and pleural invasion are mandatory.

Multivariate analysis revealed that both node involvement and pleural invasion were independent prognostic factors for recurrence in pure solid, small-sized NSCLC, though the previous study including small-sized lung cancer with GGO lesions showed a significant correlation between lymph node metastasis and pleural invasion [12]. The clinical influence of pleural invasion has been previously investigated and found to be a significant predictor of worse survival in T1 lung cancer [19]. In the soon-to-arrive TNM classification, lung cancer smaller than 2 cm is classified as T1a, though tumour invading visceral pleura is categorised as T2 [20]. The high risk of recurrence for patients with tumour invading visceral pleura (Fig. 3) provides support for the new TNM staging system, although the pleural factor was not identified as an independent predictor for OS in the present study. Pleural involvement might influence relapse rather than OS in small-sized pure solid lung cancer. Pleural invasion should be assessed using preoperative CT and given careful inspection during surgery. Macroscopically, severe pleural indentation or alteration could be considered pleural involvement and intra-operative rapid diagnosis with frozen section could be an optional to decide an extent of resection. Thus, a standard lobectomy can be recommended for pure solid, small-sized, lung cancer with pleural invasion, except in the clinical trial setting.

Radical sublobar resection requires intrapulmonary or hilar lymph node sampling during surgery to avoid underestimating nodal metastases. We usually dissect the lymph node adjacent to the segmental bronchus, which is considered to be the sentinel node of lymph drainage. The analyses of metastatic nodes according to tumour location showed the usual distribution in small-sized lung cancer;